

Lithium loss kinetics from polycrystalline $\text{Li}_x\text{Ni}_{1-x}\text{O}$ at high temperatures

Ermete Antolini

ENEA C.R. Casaccia, Via Agullarese 301, I-00060 Santa Maria di Galeria, Roma, Italy

Received 29th July 1997, Accepted 21st September 1998

Lithium loss kinetics from polycrystalline $\text{Li}_x\text{Ni}_{1-x}\text{O}$ has been investigated in the temperature range 900–1500 °C by measuring the time and temperature dependence of the weight and lattice constant change of the samples. At 900 °C the rate of Li_2O evaporation was controlled by lithium ion diffusion in $\text{Li}_x\text{Ni}_{1-x}\text{O}$. An initial region of fast diffusion followed by a region of slower diffusion was observed in the thermogravimetric measurements. This observation can be interpreted as the rapid diffusion of lithium ions along the grain boundaries and subsequent diffusion into the bulk of the grain. A plot of the logarithm of lithium loss following 2 h of thermal treatment at different temperatures vs. the reciprocal of absolute temperature consisted of two straight lines, the slope depending on the activation energy of the process and the change of slope occurred at 1300 °C. This behaviour suggests that up to 1300 °C lithium ion diffusion from the bulk to the surface of $\text{Li}_x\text{Ni}_{1-x}\text{O}$ particles was the rate-determining step. Above 1300 °C, instead, the evaporation process depended on the demixing reaction of $\text{Li}_2\text{O}(\text{g})$ and $\text{NiO}(\text{s})$ at the surface of the particles.

Pure, stoichiometric nickel oxide is a compound with cubic NaCl-type structure. Reaction of Li_2O and NiO in the presence of oxygen gives rise to the formation of $\text{Li}_x\text{Ni}_{1-x}\text{O}$ solid solution, where the oxidation state of Ni partially changes from +2 to +3.^{1,2} The unit cell slightly decreases with increasing lithium content as a consequence of the difference in the ionic radius between Ni^{2+} and Ni^{3+} ions. For lithium atomic fraction $x > 0.31$ a rhombohedral distortion of the cubic structure by lithium nickel ordering on alternate (111) planes takes place, giving rise to a hexagonal symmetry.^{2–4} $\text{Li}_x\text{Ni}_{1-x}\text{O}$ solid solutions are used as a cathode material in molten carbonate fuel cells.⁵ Moreover $\text{Li}_x\text{Ni}_{1-x}\text{O}$ has been studied with the aim of developing humidity ceramic sensors.⁶ Studies on the synthesis of $\text{Li}_x\text{Ni}_{1-x}\text{O}$ with low ($x \leq 0.23$)^{7,8} and high ($x \geq 0.30$)⁹ lithium content by solid state reaction of a Ni and Li_2CO_3 powder mixture indicated that solid solution occurs in two steps: (i) first, formation of $\text{Li}_x\text{Ni}_{1-x}\text{O}$ with x higher than the nominal value at the grain surface, then (ii) diffusion of lithium ions from the surface to the bulk of the particle.

Few studies have dealt with Li_2O evaporation from $\text{Li}_x\text{Ni}_{1-x}\text{O}$. A recent work of Sata¹⁰ on the vaporization of lithium oxide from $\text{Li}_x\text{Ni}_{1-x}\text{O}$ solid solution at temperatures up to 700 °C stated that Li_2O_2 formation and its diffusion rate in the specimen might be related to the rate-determining step in the vaporization process. Above 1000 °C, Iida found that the evaporation of lithium oxide from the solid solution is diffusion-controlled and governed by a parabolic law.¹¹ The distribution of remaining lithium ions in the solid solution following the loss of some Li_2O was also investigated. Sata found that the lithium concentration in the specimen decreased linearly from the surface to the interior along the specimen thickness.¹⁰ Azzoni *et al.*¹² observed the coexistence of substitutional solid solution NiO type and ordered solid solution LiNiO_2 type structures with different lithium content following Li_2O evaporation from ordered solid solutions ($x > 0.30$). Moreover, Berbenni *et al.*¹³ revealed structural and microstructural changes of $\text{Li}_x\text{Ni}_{1-x}\text{O}$ solid solution during Li_2O evaporation at 800 °C.

The aim of this work is to better understand the process of Li_2O evaporation from the solid solution at high temperatures in the range 900 to 1500 °C. The nominal lithium content of the composition investigated was $x = 0.30$, as for $x < 0.30$ the final amount of lithium would be very low and difficult to

detect, and for $x > 0.30$ the change of crystal structure during the evaporation process would complicate the interpretation of the results.

Experimental

Lithium nickel oxide solid solution was prepared by solid state reaction of Ni and Li_2CO_3 . Nickel powder (INCO 255) and lithium carbonate (Merck 5671) in the nominal lithium atomic fraction $x = 0.30$ were used as starting materials. This powder mixture was submitted to the following thermal treatments in air: (i) heating from room temperature to 900 °C at 1.0 K min⁻¹; (ii) isothermal treatment at 900 °C up to 40 h; (iii) heating at 3.0 K min⁻¹ from 900 °C to the maximum temperature in the range 1000–1500 °C; (iv) isothermal treatment at the maximum temperature for 2 h and (v) cooling to room temperature at 10 K min⁻¹. Moreover two samples were treated for different times at 1200 and 1400 °C, respectively.

Thermogravimetric measurements were performed using a Du Pont 2000 thermal analysis system equipped with a 951 TGA module.

XRD patterns were collected at room temperature after quenching of the samples on a Philips PW 1729 powder diffractometer equipped with a 1771 vertical goniometer using filtered Cu-K α radiation.

Results and discussion

$\text{Li}_x\text{Ni}_{1-x}\text{O}$ was formed during the dynamic step up to 900 °C of the thermal treatment. As lithium loss takes place during the process of formation of $\text{Li}_x\text{Ni}_{1-x}\text{O}$ from Ni/ Li_2CO_3 mixtures,¹⁴ we determined the lithium atomic fraction at the beginning of the isothermal step at 900 °C from both X-ray diffraction (XRD) and thermogravimetric measurements. From XRD measurements, the following relation between lithium atomic fraction x and lattice constant $a/\text{Å}$ was used:¹⁵

$$x = (4.1748 - a)/0.17756 \quad (1)$$

From the weight change, we utilised the following relation:¹⁶

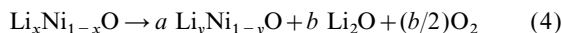
$$x = [A(1 + \Delta m/m_0) - M_{\text{NiO}}]/[A(1 + \Delta m/m_0) - (M_{\text{Ni}} - M_{\text{Li}})] \quad (2)$$

with

$$A = M_{\text{Ni}} + x_n M_{\text{Li}_2\text{CO}_3} / 2(1 - x_n) \quad (3)$$

where $\Delta m/m_0$ is the weight change of the samples, x_n is nominal lithium atomic fraction, and M_{NiO} , M_{Ni} , M_{Li} and $M_{\text{Li}_2\text{CO}_3}$ are the molecular weights of the compounds. The value of x obtained was 0.260 from XRD measurements ($a = 4.1286 \text{ \AA}$) and 0.265 from thermogravimetric measurements ($\Delta m/m_0 = 0.113$), *i.e.* the same within experimental error.

The Li_2O evaporation reaction is given by eqn. (4).



where $a = (1-x)/(1-y)$ and $b = (x-y)/2(1-y)$ for $x > y$.

This reaction takes place in two steps: (i) lithium ion diffusion to the grain surface and (ii) a demixing reaction of $\text{Li}_2\text{O}(\text{g})$ and $\text{NiO}(\text{s})$ at the surface of the particles. The basic phenomenological mass transport relation, governing a solid state diffusion process like lithium ion diffusion in $\text{Li}_x\text{Ni}_{1-x}\text{O}$, is that of Fick:

$$J = -D \text{grad } C \quad (5)$$

where J is the number of atoms crossing a unit area in unit time, C is the concentration of the mobile species, and the constant D is the chemical diffusion coefficient. In solids atoms adopt reasonably well defined positions. Mass transport occurs by atoms making transitions between these positions in such a way that the time of transit is much less than the residence time at any particular position. Thus, diffusion can be thought of as occurring by particle hopping in a random way on a lattice of sites distributed in space.¹⁷ The hopping event between sites involves the particle crossing an energy barrier, the necessary energy coming from thermal fluctuations with a probability described by the Boltzmann distribution. Hence, the diffusion process is thermally activated and the diffusion coefficient has the Arrhenius form:

$$D = D_0 \exp(-E_a/RT) \quad (6)$$

where E_a is the activation energy of diffusion. The evaporation kinetics can be expressed as:

$$C_{\text{ev}} = kt^n \quad (7)$$

where C_{ev} is the amount of evaporated species, $k = k_0 \exp(-E_a/RT)$ is the rate constant, t is the thermal treatment time and the exponent n is related to the reaction mechanism. Diffusion-controlled evaporation is described by $n = 0.5$ to 0.8 .¹⁸ Fig. 1 and 2 show normal and log-log plots of fractional lithium loss from the solid solution *vs.* thermal treatment time at 900°C , respectively. As can be seen in Fig. 2, the log-log plot breaks into two straight lines with different slopes. The slopes of these lines were 0.75 and 0.48, respectively. In both cases, a diffusion-controlled process is occurring. This result can be interpreted in terms of rapid lithium diffusion along the grain boundaries, followed by lithium diffusion into the

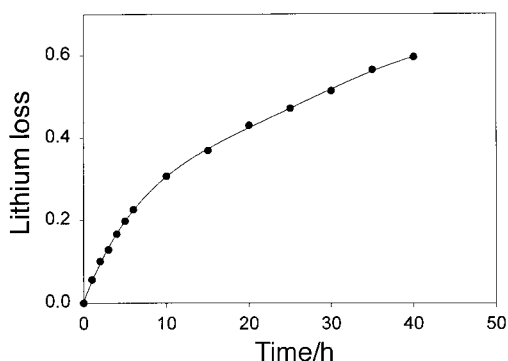


Fig. 1 Dependence of fractional lithium loss from the solid solution on thermal treatment time at 900°C .

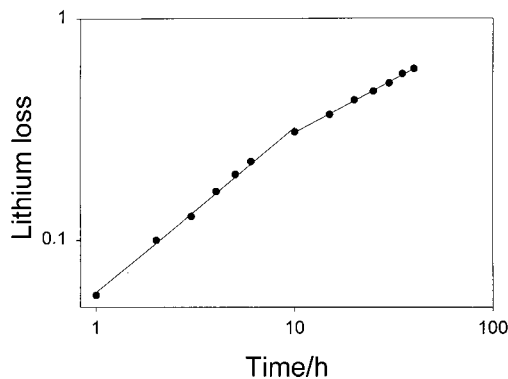


Fig. 2 Log-log plot of fractional lithium loss from the solid solution *vs.* thermal treatment time at 900°C .

grain from the bulk to the lithium-poor boundaries. Diffusion in polycrystalline solids is known to occur along grain boundaries more rapidly than through the interior of the crystals. Atkinson found that Ni diffusion in NiO was enhanced at grain boundaries with respect to lattice diffusion and that the faster diffusion pathway had the lower activation energies.¹⁹ The fast grain boundary diffusion is caused by the segregation of point defects to the core region where they have higher concentration and higher mobility than in the lattice.²⁰ As long as the rate of grain-boundary diffusion is greater than that of lattice diffusion at all temperatures, we can assume that in the diffusion controlled region not only at 900°C , but at all temperatures, lattice diffusion is initiated after the boundaries are lithium-poor owing to lithium loss by grain-boundary diffusion.

XRD measurements confirm the results of thermogravimetric measurements. Fig. 3 shows the 204 reflections of the solid solution following different thermal treatment times at 900°C . The reflection shifts towards lower angles with time, owing to lithium loss. From 0 to 3 h, we detect a broadening of the peak, attributed to a lithium concentration gradient of outer and inner parts of the grain, as a consequence of fast lithium loss at the boundaries. The result of the Rietveld refinement procedure indicated the presence of three solid solutions with $x = 0.26$, 0.24 and 0.22, respectively. A sharpening of the reflection then occurs between 3 and 20 h, related to homogenisation of the solid solution owing to the diffusion of lithium ions from the bulk to the boundaries of the particles. The transition point between grain-boundary and lattice diffusion indicates that about 30% of lithium in the solid solution is present at the grain boundaries or at layers adjacent to the grain boundaries.

After 40 h of isothermal treatment at 900°C , the lithium atomic fraction x remaining in $\text{Li}_x\text{Ni}_{1-x}\text{O}$ is 0.123. Then, these specimens were thermally treated at various temperatures for

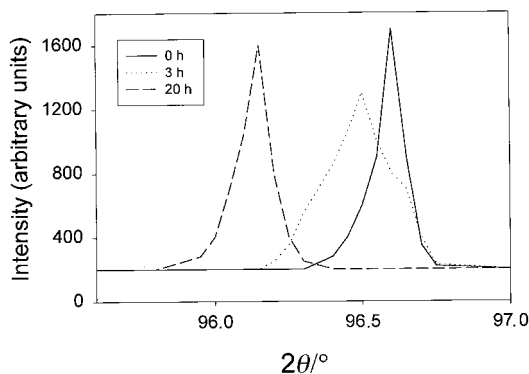


Fig. 3 Diffractometric traces of the 204 reflection of $\text{Li}_x\text{Ni}_{1-x}\text{O}$ following different times of thermal treatment at 900°C .

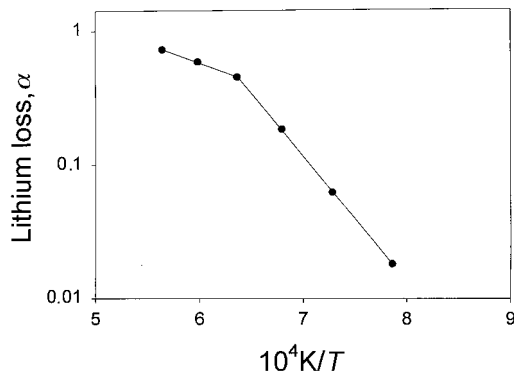


Fig. 4 The logarithm of lithium loss α from the solid solution as a function of the reciprocal of absolute temperature.

2 h. From the relation:

$$C_{ev} = k_0 \exp(-E_a/RT) t^n \quad (7)$$

plotting $\ln C_{ev}$ vs. $1/T$ at constant time, we can determine the activation energy of the process. Fig. 4 shows the dependence of the logarithm of lithium loss $\alpha = m_{Liev}/m_0Li$, (where m_{Liev} is the amount of evaporated lithium, in this case after 2 h of thermal treatment, and m_0Li is total lithium amount at the beginning of isothermal treatment) on the reciprocal of absolute temperature. A change in the slope of the plot is observed at 1300°C . This feature is related to the change of the rate-determining process. It can be inferred that at high temperatures the rate-determining step is the demixing reaction at the surface of the grain. To confirm this result we have evaluated the time-dependence of lithium loss at 1200°C (diffusion-controlled region) and 1400°C (demixing reaction-controlled region), respectively. Fig. 5 shows a plot of lithium loss $\alpha (= m_{Liev}/m_0Li)$ vs. time of samples thermally treated at 1200 and 1400°C . There are two pathways by which the rate of evaporation of Li_2O can occur at high temperature.

(a) Diffusion control: the relation of lithium loss to time is given by eqn. (8):

$$\alpha = kt^n \quad (8)$$

(b) Surface reaction: Li_2O evaporation at the grain surface follows first order kinetics [eqn. (9)]:

$$d(1-\alpha)/dt = k(1-\alpha) \quad (9)$$

Thus, the relation between lithium loss α and isothermal treatment time fits a first-order rate law [eqn. (10)]:

$$\alpha = 1 - \exp(-kt) \quad (10)$$

Fig. 6 and 7 show log-log plots of lithium loss (α) vs. time (diffusion control) and the plot of the logarithm of remaining lithium ($1-\alpha$) in the solid solution vs. time (surface reaction),

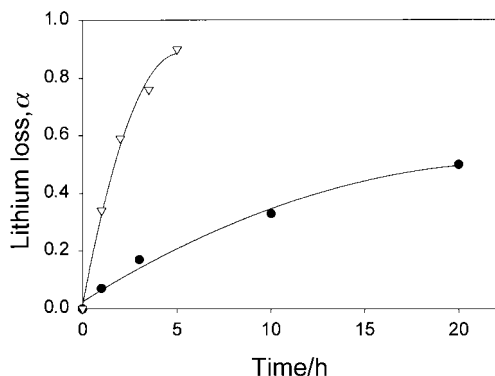


Fig. 5 Dependence of lithium loss α from the solid solution on thermal treatment time at 1200 (●) and 1400°C (▽).

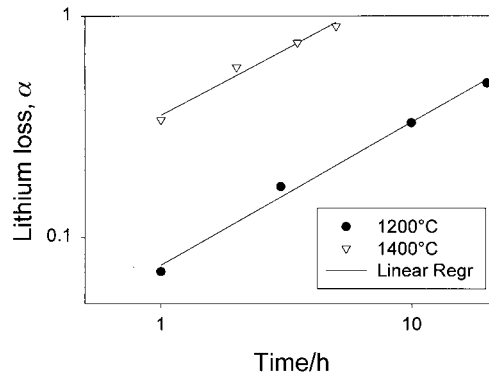


Fig. 6 Log-log plot of lithium loss α from the solid solution vs. thermal treatment time at 1200 and 1400°C .

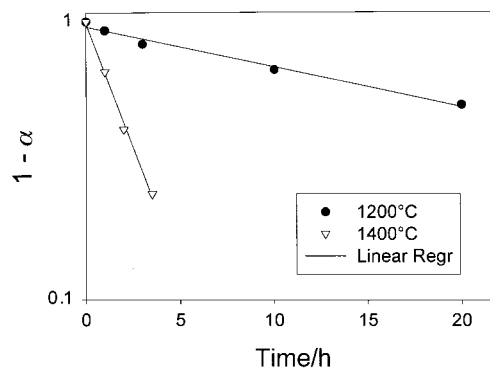


Fig. 7 Dependence of the logarithm of remaining lithium ($1-\alpha$) in the solid solution on thermal treatment time at 1200 and 1400°C .

respectively. We have determined the correlation parameters (r^2) for the experimental data and theoretical equations, the slopes of the plots shown in Fig. 6 (the slope is the value of n) and 7 (the slope is the value of k) and their estimated standard errors. As can be inferred from the values reported in Table 1, at 1200°C the best fit is shown according to the diffusion process, whereas at 1400°C the best fit is shown according to the demixing reaction at the grain surface.

The activation energy for the diffusion process was 179 kJ mol^{-1} . From the slope of $\ln[-\ln(1-\alpha)]$ vs. $1/T$, the heat of evaporation of Li_2O from $\text{Li}_x\text{Ni}_{1-x}\text{O}$ was evaluated as 92 kJ mol^{-1} .

Conclusions

In the present study it was observed that lithium loss from $\text{Li}_x\text{Ni}_{1-x}\text{O}$ with $x=0.26$ at 900°C initially occurs by grain-boundary diffusion of lithium ions in the solid solution. Then, for long times and temperatures up to 1300°C , the rate-determining step was lattice diffusion of lithium ions into $\text{Li}_x\text{Ni}_{1-x}\text{O}$. Above 1300°C , a demixing reaction of $\text{Li}_2\text{O}(\text{g})$ and $\text{NiO}(\text{s})$ at the grain surfaces was the rate-controlling step.

Table 1 Correlation parameters (r^2) of experimental data and theoretical equations, k and n values, and their estimated standard errors

Temperature/ $^\circ\text{C}$	$\log \alpha = \log k + n \log t$	$\log(1-\alpha) = -kt$
1200	$r^2=0.991$ $n=0.65$ $\Delta n/n=0.063$	$r^2=0.985$ $k=0.014 \text{ h}^{-1}$ $\Delta k/k=0.071$
1400	$r^2=0.978$ $n=0.60$ $\Delta n/n=0.103$	$r^2=0.996$ $k=0.179 \text{ h}^{-1}$ $\Delta k/k=0.042$

References

- 1 S. Van Houten, *J. Phys. Chem. Solids*, 1960, **17**, 7.
- 2 J. B. Goodenough, D. G. Wickham and W. J. Croft, *J. Phys. Chem. Solids*, 1958, **5**, 107.
- 3 I. J. Pickering, J. T. Lewandowski, A. J. Jacobson and J. A. Goldstone, *Solid State Ionics*, 1992, **53–56**, 405.
- 4 R. Stoyanova and E. Zhecheva, *J. Solid State Chem.*, 1994, **108**, 211.
- 5 *Fuel Cells Handbook*, ed. A. J. Appleby and F. R. Foulkes, Van Nostrand Reinhold, New York, 1990.
- 6 T. Sato, C. Hsien-Chang, T. Endo and M. Shimada, *J. Mater. Sci. Lett.*, 1986, **5**, 552.
- 7 E. Antolini, *J. Mater. Sci. Lett.*, 1993, **12**, 1947.
- 8 E. Antolini, A. Marini, V. Berbenni, V. Massarotti, D. Capsoni and R. Riccardi, *Solid State Ionics*, 1992, **57**, 217.
- 9 E. Antolini and M. Ferretti, *Mater. Lett.*, 1997, **30**, 59.
- 10 T. Sata, *Ceram. Int.*, 1998, **24**, 53.
- 11 Y. Iida, *J. Am. Ceram. Soc.*, 1960, **43**, 117.
- 12 C. B. Azzoni, A. Paleari, V. Massarotti, M. Bini and D. Capsoni, *Phys. Rev. B*, 1996, **53**, 703.
- 13 V. Berbenni, V. Massarotti, D. Capsoni, R. Riccardi, A. Marini and E. Antolini, *Solid State Ionics*, 1991, **48**, 101.
- 14 E. Antolini, *Mater. Lett.*, 1993, **16**, 286.
- 15 E. Antolini, M. Leonini, V. Massarotti, A. Marini, V. Berbenni and D. Capsoni, *Solid State Ionics*, 1990, **39**, 251.
- 16 A. Marini, V. Massarotti, V. Berbenni, D. Capsoni, R. Riccardi, E. Antolini and B. Passalacqua, *Solid State Ionics*, 1991, **45**, 143.
- 17 A. Atkinson, *Mater. Sci. Technol.*, 1994, **11**, 303.
- 18 T. Sata and T. Yokoyama, *Yogyo Kyokaishi*, 1973, **81**, 170.
- 19 A. Atkinson, *Adv. Ceram.*, 1987, **23**, 3.
- 20 D. M. Duffy, *J. Phys. C*, 1986, **19**, 4393.

Paper 8/05948I